

Precise Branching Ratio Measurements of the Decays $D^0 \rightarrow \pi^- \pi^+ \pi^0$ and $D^0 \rightarrow K^- K^+ \pi^0$

B. Aubert,¹ R. Barate,¹ M. Bona,¹ D. Boutigny,¹ F. Couderc,¹ Y. Karyotakis,¹ J. P. Lees,¹ V. Poireau,¹ V. Tisserand,¹ A. Zghiche,¹ E. Grauges,² A. Palano,³ J. C. Chen,⁴ N. D. Qi,⁴ G. Rong,⁴ P. Wang,⁴ Y. S. Zhu,⁴ G. Eigen,⁵ I. Ofte,⁵ B. Stugu,⁵ G. S. Abrams,⁶ M. Battaglia,⁶ D. N. Brown,⁶ J. Button-Shafer,⁶ R. N. Cahn,⁶ E. Charles,⁶ M. S. Gill,⁶ Y. Groyzman,⁶ R. G. Jacobsen,⁶ J. A. Kadyk,⁶ L. T. Kerth,⁶ Yu. G. Kolomensky,⁶ G. Kukartsev,⁶ G. Lynch,⁶ L. M. Mir,⁶ T. J. Orimoto,⁶ M. Pripstein,⁶ N. A. Roe,⁶ M. T. Ronan,⁶ W. A. Wenzel,⁶ P. del Amo Sanchez,⁷ M. Barrett,⁷ K. E. Ford,⁷ T. J. Harrison,⁷ A. J. Hart,⁷ C. M. Hawkes,⁷ S. E. Morgan,⁷ A. T. Watson,⁷ T. Held,⁸ H. Koch,⁸ B. Lewandowski,⁸ M. Pelizaeus,⁸ K. Peters,⁸ T. Schroeder,⁸ M. Steinke,⁸ J. T. Boyd,⁹ J. P. Burke,⁹ W. N. Cottingham,⁹ D. Walker,⁹ T. Cuhadar-Donszelmann,¹⁰ B. G. Fulsom,¹⁰ C. Hearty,¹⁰ N. S. Knecht,¹⁰ T. S. Mattison,¹⁰ J. A. McKenna,¹⁰ A. Khan,¹¹ P. Kyberd,¹¹ M. Saleem,¹¹ D. J. Sherwood,¹¹ L. Teodorescu,¹¹ V. E. Blinov,¹² A. D. Bukin,¹² V. P. Druzhinin,¹² V. B. Golubev,¹² A. P. Onuchin,¹² S. I. Serednyakov,¹² Yu. I. Skovpen,¹² E. P. Solodov,¹² K. Yu Todyshev,¹² D. S. Best,¹³ M. Bondioli,¹³ M. Bruinsma,¹³ M. Chao,¹³ S. Curry,¹³ I. Eschrich,¹³ D. Kirkby,¹³ A. J. Lankford,¹³ P. Lund,¹³ M. Mandelkern,¹³ R. K. Mommsen,¹³ W. Roethel,¹³ D. P. Stoker,¹³ S. Abachi,¹⁴ C. Buchanan,¹⁴ S. D. Foulkes,¹⁵ J. W. Gary,¹⁵ O. Long,¹⁵ B. C. Shen,¹⁵ K. Wang,¹⁵ L. Zhang,¹⁵ H. K. Hadavand,¹⁶ E. J. Hill,¹⁶ H. P. Paar,¹⁶ S. Rahatlou,¹⁶ V. Sharma,¹⁶ J. W. Berryhill,¹⁷ C. Campagnari,¹⁷ A. Cunha,¹⁷ B. Dahmes,¹⁷ T. M. Hong,¹⁷ D. Kovalskiy,¹⁷ J. D. Richman,¹⁷ T. W. Beck,¹⁸ A. M. Eisner,¹⁸ C. J. Flacco,¹⁸ C. A. Heusch,¹⁸ J. Kroseberg,¹⁸ W. S. Lockman,¹⁸ G. Nesom,¹⁸ T. Schalk,¹⁸ B. A. Schumm,¹⁸ A. Seiden,¹⁸ P. Spradlin,¹⁸ D. C. Williams,¹⁸ M. G. Wilson,¹⁸ J. Albert,¹⁹ E. Chen,¹⁹ A. Dvoretzki,¹⁹ F. Fang,¹⁹ D. G. Hitlin,¹⁹ I. Narsky,¹⁹ T. Piatenko,¹⁹ F. C. Porter,¹⁹ A. Ryd,¹⁹ A. Samuel,¹⁹ G. Mancinelli,²⁰ B. T. Meadows,²⁰ K. Mishra,²⁰ M. D. Sokoloff,²⁰ F. Blanc,²¹ P. C. Bloom,²¹ S. Chen,²¹ W. T. Ford,²¹ J. F. Hirschauer,²¹ A. Kreisel,²¹ M. Nagel,²¹ U. Nauenberg,²¹ A. Olivas,²¹ W. O. Ruddick,²¹ J. G. Smith,²¹ K. A. Ulmer,²¹ S. R. Wagner,²¹ J. Zhang,²¹ A. Chen,²² E. A. Eckhart,²² A. Soffer,²² W. H. Toki,²² R. J. Wilson,²² F. Winklmeier,²² Q. Zeng,²² D. D. Altenburg,²³ E. Feltresi,²³ A. Hauke,²³ H. Jasper,²³ A. Petzold,²³ B. Spaan,²³ T. Brandt,²⁴ V. Klose,²⁴ H. M. Lacker,²⁴ W. F. Mader,²⁴ R. Nogowski,²⁴ J. Schubert,²⁴ K. R. Schubert,²⁴ R. Schwierz,²⁴ J. E. Sundermann,²⁴ A. Volk,²⁴ D. Bernard,²⁵ G. R. Bonneaud,²⁵ P. Grenier,²⁵ * E. Latour,²⁵ Ch. Thiebaut,²⁵ M. Verderi,²⁵ P. J. Clark,²⁶ W. Gradl,²⁶ F. Muheim,²⁶ S. Playfer,²⁶ A. I. Robertson,²⁶ Y. Xie,²⁶ M. Andreotti,²⁷ D. Bettoni,²⁷ C. Bozzi,²⁷ R. Calabrese,²⁷ G. Cibinetto,²⁷ E. Luppi,²⁷ M. Negrini,²⁷ A. Petrella,²⁷ L. Piemontese,²⁷ E. Prencipe,²⁷ F. Anulli,²⁸ R. Baldini-Feroli,²⁸ A. Calcaterra,²⁸ R. de Sangro,²⁸ G. Finocchiaro,²⁸ S. Pacetti,²⁸ P. Patteri,²⁸ I. M. Peruzzi,²⁸ † M. Piccolo,²⁸ M. Rama,²⁸ A. Zallo,²⁸ A. Buzzo,²⁹ R. Capra,²⁹ R. Contri,²⁹ M. Lo Vetere,²⁹ M. M. Macri,²⁹ M. R. Monge,²⁹ S. Passaggio,²⁹ C. Patrignani,²⁹ E. Robutti,²⁹ A. Santroni,²⁹ S. Tosi,²⁹ G. Brandenburg,³⁰ K. S. Chaisanguanthum,³⁰ M. Morii,³⁰ J. Wu,³⁰ R. S. Dubitzky,³¹ J. Marks,³¹ S. Schenk,³¹ U. Uwer,³¹ D. J. Bard,³² W. Bhimji,³² D. A. Bowerman,³² P. D. Dauncey,³² U. Egede,³² R. L. Flack,³² J. A. Nash,³² M. B. Nikolich,³² W. Panduro Vazquez,³² P. K. Behera,³³ X. Chai,³³ M. J. Charles,³³ U. Mallik,³³ N. T. Meyer,³³ V. Ziegler,³³ J. Cochran,³⁴ H. B. Crawley,³⁴ L. Dong,³⁴ V. Eyges,³⁴ W. T. Meyer,³⁴ S. Prell,³⁴ E. I. Rosenberg,³⁴ A. E. Rubin,³⁴ A. V. Gritsan,³⁵ A. G. Denig,³⁶ M. Fritsch,³⁶ G. Schott,³⁶ N. Arnaud,³⁷ M. Davier,³⁷ G. Grosdidier,³⁷ A. Höcker,³⁷ F. Le Diberder,³⁷ V. Lepeltier,³⁷ A. M. Lutz,³⁷ A. Oyanguren,³⁷ S. Pruvot,³⁷ S. Rodier,³⁷ P. Roudeau,³⁷ M. H. Schune,³⁷ A. Stocchi,³⁷ W. F. Wang,³⁷ G. Wormser,³⁷ C. H. Cheng,³⁸ D. J. Lange,³⁸ D. M. Wright,³⁸ C. A. Chavez,³⁹ I. J. Forster,³⁹ J. R. Fry,³⁹ E. Gabathuler,³⁹ R. Gamet,³⁹ K. A. George,³⁹ D. E. Hutchcroft,³⁹ D. J. Payne,³⁹ K. C. Schofield,³⁹ C. Touramanis,³⁹ A. J. Bevan,⁴⁰ F. Di Lodovico,⁴⁰ W. Menges,⁴⁰ R. Sacco,⁴⁰ G. Cowan,⁴¹ H. U. Flaecher,⁴¹ D. A. Hopkins,⁴¹ P. S. Jackson,⁴¹ T. R. McMahon,⁴¹ S. Ricciardi,⁴¹ F. Salvatore,⁴¹ A. C. Wren,⁴¹ D. N. Brown,⁴² C. L. Davis,⁴² J. Allison,⁴³ N. R. Barlow,⁴³ R. J. Barlow,⁴³ Y. M. Chia,⁴³ C. L. Edgar,⁴³ G. D. Lafferty,⁴³ M. T. Naisbit,⁴³ J. C. Williams,⁴³ J. I. Yi,⁴³ C. Chen,⁴⁴ W. D. Hulsbergen,⁴⁴ A. Jawahery,⁴⁴ C. K. Lae,⁴⁴ D. A. Roberts,⁴⁴ G. Simi,⁴⁴ G. Blaylock,⁴⁵ C. Dallapiccola,⁴⁵ S. S. Hertzbach,⁴⁵ X. Li,⁴⁵ T. B. Moore,⁴⁵ S. Saremi,⁴⁵ H. Staengle,⁴⁵ R. Cowan,⁴⁶ G. Sciolla,⁴⁶ S. J. Sekula,⁴⁶ M. Spitznagel,⁴⁶ F. Taylor,⁴⁶ R. K. Yamamoto,⁴⁶ H. Kim,⁴⁷ S. E. Mclachlin,⁴⁷ P. M. Patel,⁴⁷ S. H. Robertson,⁴⁷ A. Lazzaro,⁴⁸ V. Lombardo,⁴⁸ F. Palombo,⁴⁸ J. M. Bauer,⁴⁹ L. Cremaldi,⁴⁹ V. Eschenburg,⁴⁹ R. Godang,⁴⁹ R. Kroeger,⁴⁹ D. A. Sanders,⁴⁹ D. J. Summers,⁴⁹ H. W. Zhao,⁴⁹ S. Brunet,⁵⁰ D. Côté,⁵⁰ M. Simard,⁵⁰ P. Taras,⁵⁰ F. B. Viaud,⁵⁰ H. Nicholson,⁵¹ N. Cavallo,⁵² ‡ G. De Nardo,⁵²

F. Fabozzi,^{52, †} C. Gatto,⁵² L. Lista,⁵² D. Monorchio,⁵² P. Paolucci,⁵² D. Piccolo,⁵² C. Sciacca,⁵² M. Baak,⁵³ G. Raven,⁵³ H. L. Snoek,⁵³ C. P. Jessop,⁵⁴ J. M. LoSecco,⁵⁴ T. Allmendinger,⁵⁵ G. Benelli,⁵⁵ K. K. Gan,⁵⁵ K. Honscheid,⁵⁵ D. Hufnagel,⁵⁵ P. D. Jackson,⁵⁵ H. Kagan,⁵⁵ R. Kass,⁵⁵ A. M. Rahimi,⁵⁵ R. Ter-Antonyan,⁵⁵ Q. K. Wong,⁵⁵ N. L. Blount,⁵⁶ J. Brau,⁵⁶ R. Frey,⁵⁶ O. Igonkina,⁵⁶ M. Lu,⁵⁶ R. Rahmat,⁵⁶ N. B. Sinev,⁵⁶ D. Strom,⁵⁶ J. Strube,⁵⁶ E. Torrence,⁵⁶ A. Gaz,⁵⁷ M. Margoni,⁵⁷ M. Morandin,⁵⁷ A. Pompili,⁵⁷ M. Posocco,⁵⁷ M. Rotondo,⁵⁷ F. Simonetto,⁵⁷ R. Stroili,⁵⁷ C. Voci,⁵⁷ M. Benayoun,⁵⁸ J. Chauveau,⁵⁸ H. Briand,⁵⁸ P. David,⁵⁸ L. Del Buono,⁵⁸ Ch. de la Vaissière,⁵⁸ O. Hamon,⁵⁸ B. L. Hartfiel,⁵⁸ M. J. J. John,⁵⁸ Ph. Leruste,⁵⁸ J. Malclès,⁵⁸ J. Ocariz,⁵⁸ L. Roos,⁵⁸ G. Therin,⁵⁸ L. Gladney,⁵⁹ J. Panetta,⁵⁹ M. Biasini,⁶⁰ R. Covarelli,⁶⁰ C. Angelini,⁶¹ G. Batignani,⁶¹ S. Bettarini,⁶¹ F. Bucci,⁶¹ G. Calderini,⁶¹ M. Carpinelli,⁶¹ R. Cenci,⁶¹ F. Forti,⁶¹ M. A. Giorgi,⁶¹ A. Lusiani,⁶¹ G. Marchiori,⁶¹ M. A. Mazur,⁶¹ M. Morganti,⁶¹ N. Neri,⁶¹ E. Paoloni,⁶¹ G. Rizzo,⁶¹ J. J. Walsh,⁶¹ M. Haire,⁶² D. Judd,⁶² D. E. Wagoner,⁶² J. Biesiada,⁶³ N. Danielson,⁶³ P. Elmer,⁶³ Y. P. Lau,⁶³ C. Lu,⁶³ J. Olsen,⁶³ A. J. S. Smith,⁶³ A. V. Telnov,⁶³ F. Bellini,⁶⁴ G. Cavoto,⁶⁴ A. D’Orazio,⁶⁴ D. del Re,⁶⁴ E. Di Marco,⁶⁴ R. Faccini,⁶⁴ F. Ferrarotto,⁶⁴ F. Ferroni,⁶⁴ M. Gaspero,⁶⁴ L. Li Gioi,⁶⁴ M. A. Mazzone,⁶⁴ S. Morganti,⁶⁴ G. Piredda,⁶⁴ F. Polci,⁶⁴ F. Safai Tehrani,⁶⁴ C. Voena,⁶⁴ M. Ebert,⁶⁵ H. Schröder,⁶⁵ R. Waldi,⁶⁵ T. Adye,⁶⁶ N. De Groot,⁶⁶ B. Franek,⁶⁶ E. O. Olaiya,⁶⁶ F. F. Wilson,⁶⁶ R. Aleksan,⁶⁷ S. Emery,⁶⁷ A. Gaidot,⁶⁷ S. F. Ganzhur,⁶⁷ G. Hamel de Monchenault,⁶⁷ W. Kozanecki,⁶⁷ M. Legendre,⁶⁷ G. Vasseur,⁶⁷ Ch. Yèche,⁶⁷ M. Zito,⁶⁷ X. R. Chen,⁶⁸ H. Liu,⁶⁸ W. Park,⁶⁸ M. V. Purohit,⁶⁸ J. R. Wilson,⁶⁸ M. T. Allen,⁶⁹ D. Aston,⁶⁹ R. Bartoldus,⁶⁹ P. Bechtle,⁶⁹ N. Berger,⁶⁹ R. Claus,⁶⁹ J. P. Coleman,⁶⁹ M. R. Convery,⁶⁹ M. Cristinziani,⁶⁹ J. C. Dingfelder,⁶⁹ J. Dorfan,⁶⁹ G. P. Dubois-Felsmann,⁶⁹ D. Dujmic,⁶⁹ W. Dunwoodie,⁶⁹ R. C. Field,⁶⁹ T. Glanzman,⁶⁹ S. J. Gowdy,⁶⁹ M. T. Graham,⁶⁹ V. Halyo,⁶⁹ C. Hast,⁶⁹ T. Hryn’ova,⁶⁹ W. R. Innes,⁶⁹ M. H. Kelsey,⁶⁹ P. Kim,⁶⁹ D. W. G. S. Leith,⁶⁹ S. Li,⁶⁹ S. Luitz,⁶⁹ V. Luth,⁶⁹ H. L. Lynch,⁶⁹ D. B. MacFarlane,⁶⁹ H. Marsiske,⁶⁹ R. Messner,⁶⁹ D. R. Muller,⁶⁹ C. P. O’Grady,⁶⁹ V. E. Ozcan,⁶⁹ A. Perazzo,⁶⁹ M. Perl,⁶⁹ T. Pulliam,⁶⁹ B. N. Ratcliff,⁶⁹ A. Roodman,⁶⁹ A. A. Salnikov,⁶⁹ R. H. Schindler,⁶⁹ J. Schwiening,⁶⁹ A. Snyder,⁶⁹ J. Stelzer,⁶⁹ D. Su,⁶⁹ M. K. Sullivan,⁶⁹ K. Suzuki,⁶⁹ S. K. Swain,⁶⁹ J. M. Thompson,⁶⁹ J. Va’vra,⁶⁹ N. van Bakel,⁶⁹ M. Weaver,⁶⁹ A. J. R. Weinstein,⁶⁹ W. J. Wisniewski,⁶⁹ M. Wittgen,⁶⁹ D. H. Wright,⁶⁹ A. K. Yarritu,⁶⁹ K. Yi,⁶⁹ C. C. Young,⁶⁹ P. R. Burchat,⁷⁰ A. J. Edwards,⁷⁰ S. A. Majewski,⁷⁰ B. A. Petersen,⁷⁰ C. Roat,⁷⁰ L. Wilden,⁷⁰ S. Ahmed,⁷¹ M. S. Alam,⁷¹ R. Bula,⁷¹ J. A. Ernst,⁷¹ V. Jain,⁷¹ B. Pan,⁷¹ M. A. Saeed,⁷¹ F. R. Wappler,⁷¹ S. B. Zain,⁷¹ W. Bugg,⁷² M. Krishnamurthy,⁷² S. M. Spanier,⁷² R. Eckmann,⁷³ J. L. Ritchie,⁷³ A. Satpathy,⁷³ C. J. Schilling,⁷³ R. F. Schwitters,⁷³ J. M. Izen,⁷⁴ X. C. Lou,⁷⁴ S. Ye,⁷⁴ F. Bianchi,⁷⁵ F. Gallo,⁷⁵ D. Gamba,⁷⁵ M. Bomben,⁷⁶ L. Bosisio,⁷⁶ C. Cartaro,⁷⁶ F. Cossutti,⁷⁶ G. Della Ricca,⁷⁶ S. Dittongo,⁷⁶ L. Lanceri,⁷⁶ L. Vitale,⁷⁶ V. Azzolini,⁷⁷ F. Martinez-Vidal,⁷⁷ Sw. Banerjee,⁷⁸ B. Bhuyan,⁷⁸ C. M. Brown,⁷⁸ D. Fortin,⁷⁸ K. Hamano,⁷⁸ R. Kowalewski,⁷⁸ I. M. Nugent,⁷⁸ J. M. Roney,⁷⁸ R. J. Sobie,⁷⁸ J. J. Back,⁷⁹ P. F. Harrison,⁷⁹ T. E. Latham,⁷⁹ G. B. Mohanty,⁷⁹ M. Pappagallo,⁷⁹ H. R. Band,⁸⁰ X. Chen,⁸⁰ B. Cheng,⁸⁰ S. Dasu,⁸⁰ M. Datta,⁸⁰ K. T. Flood,⁸⁰ J. J. Hollar,⁸⁰ P. E. Kutter,⁸⁰ B. Mellado,⁸⁰ A. Mihalyi,⁸⁰ Y. Pan,⁸⁰ M. Pierini,⁸⁰ R. Prepost,⁸⁰ S. L. Wu,⁸⁰ Z. Yu,⁸⁰ and H. Neal⁸¹

(The BABAR Collaboration)

¹Laboratoire de Physique des Particules, F-74941 Annecy-le-Vieux, France

²Universitat de Barcelona, Facultat de Física Dept. ECM, E-08028 Barcelona, Spain

³Università di Bari, Dipartimento di Fisica and INFN, I-70126 Bari, Italy

⁴Institute of High Energy Physics, Beijing 100039, China

⁵University of Bergen, Institute of Physics, N-5007 Bergen, Norway

⁶Lawrence Berkeley National Laboratory and University of California, Berkeley, California 94720, USA

⁷University of Birmingham, Birmingham, B15 2TT, United Kingdom

⁸Ruhr Universität Bochum, Institut für Experimentalphysik 1, D-44780 Bochum, Germany

⁹University of Bristol, Bristol BS8 1TL, United Kingdom

¹⁰University of British Columbia, Vancouver, British Columbia, Canada V6T 1Z1

¹¹Brunel University, Uxbridge, Middlesex UB8 3PH, United Kingdom

¹²Budker Institute of Nuclear Physics, Novosibirsk 630090, Russia

¹³University of California at Irvine, Irvine, California 92697, USA

¹⁴University of California at Los Angeles, Los Angeles, California 90024, USA

¹⁵University of California at Riverside, Riverside, California 92521, USA

¹⁶University of California at San Diego, La Jolla, California 92093, USA

¹⁷University of California at Santa Barbara, Santa Barbara, California 93106, USA

¹⁸University of California at Santa Cruz, Institute for Particle Physics, Santa Cruz, California 95064, USA

¹⁹California Institute of Technology, Pasadena, California 91125, USA

²⁰University of Cincinnati, Cincinnati, Ohio 45221, USA

- ²¹ University of Colorado, Boulder, Colorado 80309, USA
- ²² Colorado State University, Fort Collins, Colorado 80523, USA
- ²³ Universität Dortmund, Institut für Physik, D-44221 Dortmund, Germany
- ²⁴ Technische Universität Dresden, Institut für Kern- und Teilchenphysik, D-01062 Dresden, Germany
- ²⁵ Ecole Polytechnique, Laboratoire Leprince-Ringuet, F-91128 Palaiseau, France
- ²⁶ University of Edinburgh, Edinburgh EH9 3JZ, United Kingdom
- ²⁷ Università di Ferrara, Dipartimento di Fisica and INFN, I-44100 Ferrara, Italy
- ²⁸ Laboratori Nazionali di Frascati dell'INFN, I-00044 Frascati, Italy
- ²⁹ Università di Genova, Dipartimento di Fisica and INFN, I-16146 Genova, Italy
- ³⁰ Harvard University, Cambridge, Massachusetts 02138, USA
- ³¹ Universität Heidelberg, Physikalisches Institut, Philosophenweg 12, D-69120 Heidelberg, Germany
- ³² Imperial College London, London, SW7 2AZ, United Kingdom
- ³³ University of Iowa, Iowa City, Iowa 52242, USA
- ³⁴ Iowa State University, Ames, Iowa 50011-3160, USA
- ³⁵ Johns Hopkins University, Baltimore, Maryland 21218, USA
- ³⁶ Universität Karlsruhe, Institut für Experimentelle Kernphysik, D-76021 Karlsruhe, Germany
- ³⁷ Laboratoire de l'Accélérateur Linéaire, IN2P3-CNRS et Université Paris-Sud 11, Centre Scientifique d'Orsay, B.P. 34, F-91898 ORSAY Cedex, France
- ³⁸ Lawrence Livermore National Laboratory, Livermore, California 94550, USA
- ³⁹ University of Liverpool, Liverpool L69 7ZE, United Kingdom
- ⁴⁰ Queen Mary, University of London, E1 4NS, United Kingdom
- ⁴¹ University of London, Royal Holloway and Bedford New College, Egham, Surrey TW20 0EX, United Kingdom
- ⁴² University of Louisville, Louisville, Kentucky 40292, USA
- ⁴³ University of Manchester, Manchester M13 9PL, United Kingdom
- ⁴⁴ University of Maryland, College Park, Maryland 20742, USA
- ⁴⁵ University of Massachusetts, Amherst, Massachusetts 01003, USA
- ⁴⁶ Massachusetts Institute of Technology, Laboratory for Nuclear Science, Cambridge, Massachusetts 02139, USA
- ⁴⁷ McGill University, Montréal, Québec, Canada H3A 2T8
- ⁴⁸ Università di Milano, Dipartimento di Fisica and INFN, I-20133 Milano, Italy
- ⁴⁹ University of Mississippi, University, Mississippi 38677, USA
- ⁵⁰ Université de Montréal, Physique des Particules, Montréal, Québec, Canada H3C 3J7
- ⁵¹ Mount Holyoke College, South Hadley, Massachusetts 01075, USA
- ⁵² Università di Napoli Federico II, Dipartimento di Scienze Fisiche and INFN, I-80126, Napoli, Italy
- ⁵³ NIKHEF, National Institute for Nuclear Physics and High Energy Physics, NL-1009 DB Amsterdam, The Netherlands
- ⁵⁴ University of Notre Dame, Notre Dame, Indiana 46556, USA
- ⁵⁵ Ohio State University, Columbus, Ohio 43210, USA
- ⁵⁶ University of Oregon, Eugene, Oregon 97403, USA
- ⁵⁷ Università di Padova, Dipartimento di Fisica and INFN, I-35131 Padova, Italy
- ⁵⁸ Universités Paris VI et VII, Laboratoire de Physique Nucléaire et de Hautes Energies, F-75252 Paris, France
- ⁵⁹ University of Pennsylvania, Philadelphia, Pennsylvania 19104, USA
- ⁶⁰ Università di Perugia, Dipartimento di Fisica and INFN, I-06100 Perugia, Italy
- ⁶¹ Università di Pisa, Dipartimento di Fisica, Scuola Normale Superiore and INFN, I-56127 Pisa, Italy
- ⁶² Prairie View A&M University, Prairie View, Texas 77446, USA
- ⁶³ Princeton University, Princeton, New Jersey 08544, USA
- ⁶⁴ Università di Roma La Sapienza, Dipartimento di Fisica and INFN, I-00185 Roma, Italy
- ⁶⁵ Universität Rostock, D-18051 Rostock, Germany
- ⁶⁶ Rutherford Appleton Laboratory, Chilton, Didcot, Oxon, OX11 0QX, United Kingdom
- ⁶⁷ DSM/Dapnia, CEA/Saclay, F-91191 Gif-sur-Yvette, France
- ⁶⁸ University of South Carolina, Columbia, South Carolina 29208, USA
- ⁶⁹ Stanford Linear Accelerator Center, Stanford, California 94309, USA
- ⁷⁰ Stanford University, Stanford, California 94305-4060, USA
- ⁷¹ State University of New York, Albany, New York 12222, USA
- ⁷² University of Tennessee, Knoxville, Tennessee 37996, USA
- ⁷³ University of Texas at Austin, Austin, Texas 78712, USA
- ⁷⁴ University of Texas at Dallas, Richardson, Texas 75083, USA
- ⁷⁵ Università di Torino, Dipartimento di Fisica Sperimentale and INFN, I-10125 Torino, Italy
- ⁷⁶ Università di Trieste, Dipartimento di Fisica and INFN, I-34127 Trieste, Italy
- ⁷⁷ IFIC, Universitat de Valencia-CSIC, E-46071 Valencia, Spain
- ⁷⁸ University of Victoria, Victoria, British Columbia, Canada V8W 3P6
- ⁷⁹ Department of Physics, University of Warwick, Coventry CV4 7AL, United Kingdom
- ⁸⁰ University of Wisconsin, Madison, Wisconsin 53706, USA
- ⁸¹ Yale University, New Haven, Connecticut 06511, USA
- (Dated: July 27, 2021)

Using 232 fb^{-1} of e^+e^- collision data recorded by the *BABAR* experiment, we measure the rates of three-body Cabibbo-suppressed decays of the D^0 meson relative to the Cabibbo-favored decay: $\frac{B(D^0 \rightarrow \pi^- \pi^+ \pi^0)}{B(D^0 \rightarrow K^- \pi^+ \pi^0)} = (10.59 \pm 0.06 \pm 0.13) \times 10^{-2}$ and $\frac{B(D^0 \rightarrow K^- K^+ \pi^0)}{B(D^0 \rightarrow K^- \pi^+ \pi^0)} = (2.37 \pm 0.03 \pm 0.04) \times 10^{-2}$, where the errors are statistical and systematic, respectively. The precisions of these measurements are significantly better than those of the current world average values.

PACS numbers: 13.25.Ft, 12.15.Hh, 11.30.Er

Cabibbo-suppressed charm decays offer good laboratory for studying weak interactions as they provide a unique window on new physics affecting decay-rate dynamics and CP violation. The branching ratios of the singly Cabibbo-suppressed decays of D^0 meson are anomalous since the $D^0 \rightarrow \pi^- \pi^+$ branching fraction is observed to be suppressed relative to the $D^0 \rightarrow K^- K^+$ by a factor of almost three, even though the phase space for the former is larger [1]. The branching ratios of the three-body decays [2, 3] have larger uncertainties but do not appear to exhibit the same suppression. This motivates the current study which measures the branching ratios of $D^0 \rightarrow \pi^- \pi^+ \pi^0$ and $K^- K^+ \pi^0$ with respect to the Cabibbo-favored decay $D^0 \rightarrow K^- \pi^+ \pi^0$ [4].

This analysis uses a data sample corresponding to an integrated luminosity of 232 fb^{-1} of e^+e^- collisions collected around $\sqrt{s} \approx 10 \text{ GeV}$ with the *BABAR* detector [5] at the PEP-II asymmetric-energy storage rings. Tracking of charged particles is provided by a five-layer silicon vertex tracker (SVT) and a 40-layer drift chamber (DCH). Particle identification (PID) is provided by a likelihood-based algorithm which uses ionization energy loss in the DCH and SVT, and Cherenkov photons detected in a ring-imaging detector (DIRC). A large control sample of $D^{*+} \rightarrow D^0(K^- \pi^+) \pi_s^+$ events is used to evaluate PID performance for kaons and pions from data. The average identification efficiencies and the misidentification rates for pions (kaons) are 95% (90%) and 1% (3%) respectively. The typical separation between pions and kaons varies from 8 standard deviations (σ) at momenta of $2 \text{ GeV}/c$ to 2.5σ at $4 \text{ GeV}/c$. An electromagnetic calorimeter (EMC) is used to identify electrons and photons. These systems are mounted inside a 1.5-T solenoidal magnet. The GEANT4 package [6] is used to simulate the response of the detector with varying accelerator and detector conditions. Event reconstruction efficiency is obtained using Monte Carlo (MC) simulated events having production characteristics from the JET-SET [7] fragmentation algorithm. Three-body D^0 decays are generated with uniform Dalitz plot [8] (phase space) distributions. Electromagnetic radiation from final state charged particles (FSR) is modeled using the PHOTOS package [9].

To reduce combinatorial backgrounds, we reconstruct D^0 candidates in decays $D^{*+} \rightarrow D^0 \pi_s^+$ (π_s^+ is a soft, low momentum charged pion) with $D^0 \rightarrow K^- \pi^+ \pi^0$, $\pi^- \pi^+ \pi^0$, and $K^- K^+ \pi^0$, by selecting events with at least three charged tracks and a neutral pion. Photon candidates

are reconstructed from calorimeter energy deposits above 100 MeV, which are not matched to charged tracks. Neutral pions are reconstructed from pairs of photons with an invariant mass in the range 115–160 MeV/c^2 and total energy in the laboratory system above 350 MeV. Charged kaon and pion and π_s^+ candidate tracks are required to be within the fiducial volumes of the tracking and PID systems; they must have at least 20 hits in the DCH and transverse momenta greater than 0.1 GeV/c . Also, they must pass PID selection criteria.

To form a D^0 candidate, two oppositely charged tracks and π^0 are fit to a common vertex, constraining the $\gamma\gamma$ invariant mass to the nominal π^0 mass. The invariant mass of the D^0 candidate after the vertex fit is required to lie in the range 1.7–2.0 GeV/c^2 . To reduce high multiplicity events and combinatorial backgrounds, the momentum of the D^0 candidate in the event's center-of-mass frame (p^*) is required to be greater than 2.77 GeV/c (this requirement also ensures that D^0 candidates from B decay are removed). The selected candidates after the above requirements are combined with the π_s^+ track to form a D^{*+} candidate. The D^0 and the π_s^+ are constrained to originate from the collision point; the resolution in Δm , defined as the difference in invariant masses of the D^{*+} and D^0 candidates, is approximately 0.3 MeV/c^2 for all three modes. Only those candidates are retained for which the vertex fit to the whole decay chain has a χ^2 probability greater than 0.01 and Δm is in the range 144.9–146.1 MeV/c^2 . At this stage, approximately 3% of the events have multiple $D^{*+} \rightarrow D^0 \pi_s^+$ candidates satisfying our selection criteria, due to D^0 misreconstruction or a correctly reconstructed D^0 combining with a fake π_s . When there is more than one candidate in an event, we select only the candidate with the lowest vertex fit χ^2 . Our selection procedures result in $K^- \pi^+ \pi^0$, $\pi^- \pi^+ \pi^0$, and $K^- K^+ \pi^0$ samples with purities 99%, 95% and 96%, respectively.

The number of D^0 signal events in each decay mode is obtained by fitting the observed D^0 candidate mass distribution to the sum of signal and background components, where the latter has combinatorial contributions and reflection contributions from real three-body D^0 decays where a kaon (pion) is misidentified as a pion (kaon). The signal component is described by a sum of three Gaussians whose means and widths are allowed to vary. The combinatorial background is modeled by a linear function. According to the MC simulation, a large fraction of the background consists of $e^+e^- \rightarrow c\bar{c}$ events,

with small contributions from processes $e^+e^- \rightarrow b\bar{b}$, $u\bar{u}$, $d\bar{d}$, $s\bar{s}$. Reflected $K^-\pi^+\pi^0$ events peak in the lower (upper) sideband of $m_{\pi^-\pi^+\pi^0}$ ($m_{K^-K^+\pi^0}$). The levels of various background contributions in the $\pi^-\pi^+\pi^0$ and the $K^-K^+\pi^0$ invariant mass distributions are shown in Fig. 1. The shapes of the $K^-\pi^+\pi^0$ reflections in the $\pi^-\pi^+\pi^0$ and $K^-K^+\pi^0$ invariant mass distributions are obtained from MC. The numbers of reflected events are found by making the $K^-\pi^+\pi^0$ invariant mass distributions for the $\pi^-\pi^+\pi^0$ and $K^-K^+\pi^0$ samples and fitting them. Finally, maximum-likelihood fits are performed to extract the signal yields from the data for each of the three modes. The $D^0 \rightarrow K_S^0\pi^0$ decay is a Cabibbo-favored decay and a background for the $D^0 \rightarrow \pi^-\pi^+\pi^0$ mode. The level of this contamination is obtained by fitting the K_S^0 peak in the $m_{\pi^-\pi^+}$ distribution and the number of $K_S^0\pi^0$ events is subtracted from the $\pi^-\pi^+\pi^0$ signal yield. The fitted D^0 candidate mass plots for the three modes are shown in Fig. 2 and the results of the fits are reported in Table I.

The event reconstruction efficiency is obtained from

| Mode | Number of signal events (S) | Central value of D^0 mass (GeV/c^2) | Resolution (MeV/c^2) |
|-------------------|---------------------------------|--|---------------------------------|
| $K^-\pi^+\pi^0$ | 505660 ± 750 | 1.8646 ± 0.0002 | 16.0 ± 0.5 |
| $\pi^-\pi^+\pi^0$ | 60426 ± 343 | 1.8637 ± 0.0004 | 17.4 ± 0.8 |
| $K^-K^+\pi^0$ | 10773 ± 122 | 1.8649 ± 0.0004 | 13.5 ± 1.0 |

TABLE I: Number of observed signal events and the central value and resolution of the D^0 candidate mass distribution obtained from fit. The central value and the resolution are, respectively, the average mean and rms width of three Gaussians in the signal weighted by their fit-fractions. The errors are statistical only.

MC. The reconstruction efficiency for each event is calculated as a function of its position in the D^0 Dalitz plot. That position is calculated using track momenta from a fit which constrains the $h^-h^+\pi^0$ invariant mass to be the nominal D^0 mass, where ‘h’ is either a kaon or a pion. To correct for the differences in PID efficiency in data and MC, the ratio of these is determined for each track in bins of momentum and polar angle, and an event-by-event PID-correction factor is applied to each reconstructed event. The inverse of the calculated efficiency for each data point is taken as its weight. The average weight for each decay mode is computed by summing the weights of all events in the nominal signal regions ($\pm 3\sigma$ around the observed mean values of the D^0 mass distributions) and subtracting the efficiency-corrected event yields from sidebands (1.75–1.79 GeV/c^2 and 1.95–1.99 GeV/c^2 , spaced almost symmetrically around the nominal D^0 mass) to account for background events in the signal region. For the $K^-\pi^+\pi^0$ mode both sidebands are used for this purpose; for the $\pi^-\pi^+\pi^0$ ($K^-K^+\pi^0$) mode only the upper (lower) sideband is used because of the $K^-\pi^+\pi^0$ reflection in the other sideband. The average

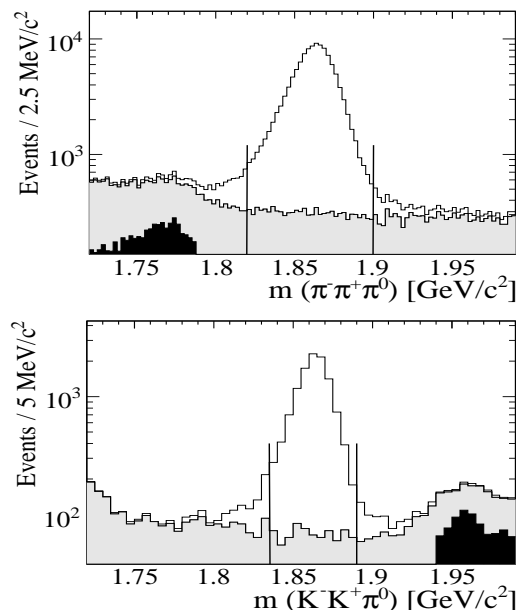


FIG. 1: Simulated $\pi^-\pi^+\pi^0$ (top) and $K^-K^+\pi^0$ (bottom) invariant mass distributions. Signal events are shown as open histograms. Combinatorial and reflection backgrounds are shown by the light and dark shaded histograms, respectively. The signal region is delimited by the vertical lines.

weights obtained from this method are verified to be unbiased. The average reconstruction weights for $K^-\pi^+\pi^0$, $\pi^-\pi^+\pi^0$, and $K^-K^+\pi^0$ modes are 10.75 ± 0.02 , 9.43 ± 0.02 , and 12.61 ± 0.05 respectively, where the uncertainty is due to MC statistics.

The branching ratios are obtained from

$$\frac{B(D^0 \rightarrow \pi^-\pi^+\pi^0)}{B(D^0 \rightarrow K^-\pi^+\pi^0)} = \frac{N_{\pi^-\pi^+\pi^0} \times W_{\pi^-\pi^+\pi^0}}{N_{K^-\pi^+\pi^0} \times W_{K^-\pi^+\pi^0}}, \quad (1)$$

$$\frac{B(D^0 \rightarrow K^-K^+\pi^0)}{B(D^0 \rightarrow K^-\pi^+\pi^0)} = \frac{N_{K^-K^+\pi^0} \times W_{K^-K^+\pi^0}}{N_{K^-\pi^+\pi^0} \times W_{K^-\pi^+\pi^0}}, \quad (2)$$

where N and W stand for the number of signal events detected and the average weight, respectively.

The most important sources of systematic uncertainties in the branching ratios are reported in Table II. The finite statistics of the MC samples used to obtain reconstruction efficiencies contributes a small uncertainty. The uncertainty due to the Δm selection is estimated by repeating the analysis with different selection windows. The systematic uncertainty due to the background subtraction procedure is obtained by repeating the analysis using $c\bar{c}$ Monte Carlo data and subtracting identifiable ‘‘true’’ background events in the signal region. The uncertainty caused by Dalitz plot binning effects in the efficiency calculation is estimated by varying the bin-size. The effect of the modeling of the background probability distribution function on the signal yield is studied

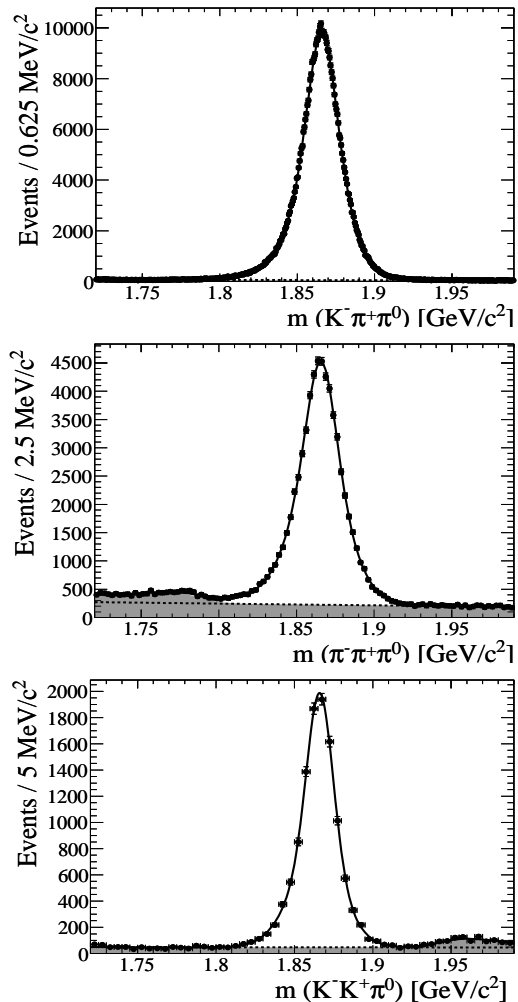


FIG. 2: Fitted mass for the $K^-\pi^+\pi^0$, $\pi^-\pi^+\pi^0$, and $K^-K^+\pi^0$ data samples. Dots are data points and the solid curves are the fit. The dot-dashed lines show the level of combinatorial background in each case. For the $\pi^-\pi^+\pi^0$ and the $K^-K^+\pi^0$ modes, the shaded region represents the total background.

by repeating the fits to the D^0 candidate mass distributions with exponential and polynomial combinatorial background models. The systematic effect due to differences in the p^* distribution in data and MC was determined by correcting the reconstruction efficiency obtained from MC by the ratio of p^* distributions in data and MC. Charged-particle identification studies in the data lead to small corrections applied to each track in the simulation. A large control sample of data and MC is studied separately to determine the residual PID uncertainties. Uncertainty due to potential differences in charged-particle tracking efficiencies in data and MC originating from an imprecise knowledge of different kaon and pion nuclear interaction cross sections and from the approximations used in our material model simulation, is conservatively assigned.

As a consistency check, the analysis is performed sep-

| Systematics | $\frac{B(D^0 \rightarrow \pi^-\pi^+\pi^0)}{B(D^0 \rightarrow K^-\pi^+\pi^0)}$ | $\frac{B(D^0 \rightarrow K^-K^+\pi^0)}{B(D^0 \rightarrow K^-\pi^+\pi^0)}$ |
|----------------------|---|---|
| | MC statistics | 0.27% |
| Δm selection | 0.30% | 0.90% |
| Bg. Subtraction | 0.60% | 0.90% |
| Efficiency binning | 0.11% | 0.24% |
| Bg. PDF model | 0.16% | 0.13% |
| p^* difference | 0.24% | 0.02% |
| PID | 0.77% | 0.84% |
| Tracking | 0.60% | 0.60% |
| K_S^0 Removal | 0.07% | — |
| Total | 1.25% | 1.73% |

TABLE II: Summary of systematic uncertainties. The total systematic uncertainty was obtained by adding the individual contributions in quadrature.

arately for D^0 and \bar{D}^0 events in different ranges of the D^0 candidate laboratory momenta to look for systematic variations as a function of charge or momentum outside the levels accounted for in the estimation of statistical and systematic uncertainties. The analysis is repeated for different data run periods and on the MC sample treated as data. As yet another cross-check, the branching ratios are measured by directly fitting the efficiency-corrected histograms of the D^0 invariant mass distributions and then taking the ratio of the yields obtained from the fit. The results from all these cross-checks are consistent with the results of the main analysis.

Using equations 1 and 2, we obtain the following results for the branching ratios:

$$\frac{B(D^0 \rightarrow \pi^-\pi^+\pi^0)}{B(D^0 \rightarrow K^-\pi^+\pi^0)} = (10.59 \pm 0.06 \pm 0.13) \times 10^{-2}, \quad (3)$$

$$\frac{B(D^0 \rightarrow K^-K^+\pi^0)}{B(D^0 \rightarrow K^-\pi^+\pi^0)} = (2.37 \pm 0.03 \pm 0.04) \times 10^{-2}, \quad (4)$$

where the errors are statistical and systematic, respectively. The previous most precise measurements for these branching ratios are $(8.40 \pm 3.11) \times 10^{-2}$ and $(0.95 \pm 0.26) \times 10^{-2}$, respectively [10]. We note that the second result differs significantly from the current world average value. As we consider events with any level of FSR as parts of our signals, the ratios we measure correspond to those of the so-called “bare” decay rates discussed, for example, in Ref. [11]. Using the world average value [1] for the $D^0 \rightarrow K^-\pi^+\pi^0$ branching fraction, we obtain,

$$B(D^0 \rightarrow \pi^-\pi^+\pi^0) = (1.493 \pm 0.008 \pm 0.018 \pm 0.053) \times 10^{-2}, \quad (5)$$

$$B(D^0 \rightarrow K^-K^+\pi^0) = (0.334 \pm 0.004 \pm 0.006 \pm 0.012) \times 10^{-2}, \quad (6)$$

where the errors are statistical, systematic, and due to the uncertainty of $B(D^0 \rightarrow K^- \pi^+ \pi^0)$.

The decay rate for each process can be written as:

$$\Gamma = \int d\Phi |\mathcal{M}|^2, \quad (7)$$

where Γ is the decay rate to a particular three-body final state, \mathcal{M} is the decay matrix element, and Φ is the phase space. Integrating over the Dalitz plot assuming a uniform phase space density, the above equation can be written as:

$$\Gamma = \langle |\mathcal{M}|^2 \rangle \times \Phi, \quad (8)$$

where $\langle |\mathcal{M}|^2 \rangle$ is the average value of $|\mathcal{M}|^2$ over the Dalitz plot and the three-body phase space, Φ is proportional to the area of the Dalitz plot. For the three signal decays Φ is in the ratio $\pi^- \pi^+ \pi^0 : K^- \pi^+ \pi^0 : K^- K^+ \pi^0 = 5.05 : 3.19 : 1.67$. Combining the statistical and systematic errors, we find:

$$\frac{\langle |\mathcal{M}|^2 \rangle (D^0 \rightarrow \pi^- \pi^+ \pi^0)}{\langle |\mathcal{M}|^2 \rangle (D^0 \rightarrow K^- \pi^+ \pi^0)} = (6.68 \pm 0.04 \pm 0.08) \times 10^{-2} \quad (9)$$

$$\frac{\langle |\mathcal{M}|^2 \rangle (D^0 \rightarrow K^- K^+ \pi^0)}{\langle |\mathcal{M}|^2 \rangle (D^0 \rightarrow K^- \pi^+ \pi^0)} = (4.53 \pm 0.06 \pm 0.08) \times 10^{-2} \quad (10)$$

$$\frac{\langle |\mathcal{M}|^2 \rangle (D^0 \rightarrow K^- K^+ \pi^0)}{\langle |\mathcal{M}|^2 \rangle (D^0 \rightarrow \pi^- \pi^+ \pi^0)} = (6.78 \pm 0.14 \pm 0.21) \times 10^{-1}. \quad (11)$$

To the extent that the differences in the matrix elements are only due to Cabibbo-suppression at the quark level, the ratios of the matrix elements squared for singly Cabibbo-suppressed decays to that for the Cabibbo-favored decay should be approximately $\sin^2 \theta_C \approx 0.05$ and the ratio of the matrix elements squared for the two singly Cabibbo-suppressed decays should be unity. The deviations from this naive picture are less than 35% for these three-body decays. In contrast, the corresponding ratios may be calculated for the two-body decays $D^0 \rightarrow \pi^- \pi^+$, $D^0 \rightarrow K^- \pi^+$, and $D^0 \rightarrow K^- K^+$. Using the world average values for two-body branching ratios [1], the ratios of the matrix elements squared for two-body Cabibbo-suppressed decays, corresponding to Eqs. 9–11, are, respectively, 0.034 ± 0.001 , 0.111 ± 0.002 , and 3.53 ± 0.12 . Thus the naive Cabibbo-suppression model works well for three-body decays but not so well for two-body decays.

In summary, we have measured the ratios of the decay rates for the three-body singly Cabibbo-suppressed decays $D^0 \rightarrow \pi^- \pi^+ \pi^0$ and $D^0 \rightarrow K^- K^+ \pi^0$ relative to that for the Cabibbo-favored decay $D^0 \rightarrow K^- \pi^+ \pi^0$. This constitutes the most precise measurement for these channels

to date. The average squared matrix elements for both of the singly Cabibbo-suppressed decays are roughly a factor of $\sin^2 \theta_C$ smaller than that for the Cabibbo-favored decay and are therefore, in contrast to the corresponding two-body modes, consistent with the naive expectations.

We are grateful for the extraordinary contributions of our PEP-II colleagues in achieving the excellent luminosity and machine conditions that have made this work possible. The success of this project also relies critically on the expertise and dedication of the computing organizations that support *BABAR*. The collaborating institutions wish to thank SLAC for its support and the kind hospitality extended to them. This work is supported by the US Department of Energy and National Science Foundation, the Natural Sciences and Engineering Research Council (Canada), Institute of High Energy Physics (China), the Commissariat à l’Energie Atomique and Institut National de Physique Nucléaire et de Physique des Particules (France), the Bundesministerium für Bildung und Forschung and Deutsche Forschungsgemeinschaft (Germany), the Istituto Nazionale di Fisica Nucleare (Italy), the Foundation for Fundamental Research on Matter (The Netherlands), the Research Council of Norway, the Ministry of Science and Technology of the Russian Federation, Ministerio de Educación y Ciencia (Spain), and the Particle Physics and Astronomy Research Council (United Kingdom). Individuals have received support from the Marie-Curie IEF program (European Union) and the A. P. Sloan Foundation.

* Also at Laboratoire de Physique Corpusculaire, Clermont-Ferrand, France

† Also with Università di Perugia, Dipartimento di Fisica, Perugia, Italy

‡ Also with Università della Basilicata, Potenza, Italy

- [1] Particle Data Group, W. M. Yao *et al.*, *J. Phys. G* **33**, 1 (2006).
- [2] R. M. Baltrusaitis *et al.*, *Phys. Rev. Lett.* **55**, 150153 (1985).
- [3] CLEO Collaboration, D. M. Asner *et al.*, *Phys. Rev. D* **54**, 4211 (1996).
- [4] Reference to the charge-conjugate decays is implied throughout the text, unless stated otherwise.
- [5] *BABAR* Collaboration, B. Aubert *et al.*, *Nucl. Instr. and Methods* **A479**, 1 (2002).
- [6] GEANT4 Collaboration, S. Agostinelli *et al.*, *Nucl. Instr. and Methods* **A506**, 250 (2003).
- [7] T. Sjostrand *et al.*, *Comput. Phys. Commun.* **135**, 238 (2001).
- [8] R. H. Dalitz, *Phil. Mag.* **44**, 1068 (1953).
- [9] E. Barberio and Z. Was, *Comput. Phys. Commun.* **79**, 291 (1994).
- [10] The CLEO Collaboration (P. Rubin *et al.*, *Phys. Rev. Lett.* **96**, 081802 (2006)) has measured the branching ratio of $D^0 \rightarrow \pi^- \pi^+ \pi^0$ relative to $D^0 \rightarrow K^- \pi^+$ decay.
- [11] E. Baracchini and G. Isidori, *Phys. Lett. B* **633**, 309

(2006).